Gastroenterology 2021;160:847–862

Regeneration Defects in *Yap* and *Taz* Mutant Mouse Livers Are Caused by Bile Duct Disruption and Cholestasis

Elisabeth Verboven,[1] Iván M. Moya,[1,2] Leticia Sansores-Garcia,[1] Jun Xie,[1] Hanne Hillen,[1] Weronika Kowalczyk,[1] Gerlanda Vella,[1] Stefaan Verhulst,[3] Stéphanie A. Castaldo,[1] Ana Algueró-Nadal,[1] Lucia Romanelli,[1] Cristina Mercader-Celma,[1] Natália A. Souza,[1] Soheil Soheily,[1] Leen Van Huffel,[1] Thomas Van Brussel,[1] Diether Lambrechts,[1] Tania Roskams,[4] Frédéric P. Lemaigre,[5] Gabrielle Bergers,[1] Leo A. van Grunsven,[3] and Georg Halder[1]

[1]Vlaams Instituut voor Biotechnologie-Katholieke Universiteit Leuven, Center for Cancer Biology, Department of Oncology, Katholieke Universiteit Leuven, Leuven, Belgium; [2]Facultad de Ingeniería y Ciencias Aplicadas, Universidad de Las Americas, Quito, Ecuador; [3]Liver Cell Biology Research Group, Faculty of Medicine and Pharmacy, Vrije Universiteit Brussel, Brussel, Belgium; [4]Department of Imaging and Pathology, Translational Cell and Tissue Research, Katholieke Universiteit Leuven and University Hospitals Leuven, Leuven, Belgium; and [5]Liver and Pancreas Development Unit, de Duve Institute, Université catholique de Louvain, Brussels, Belgium

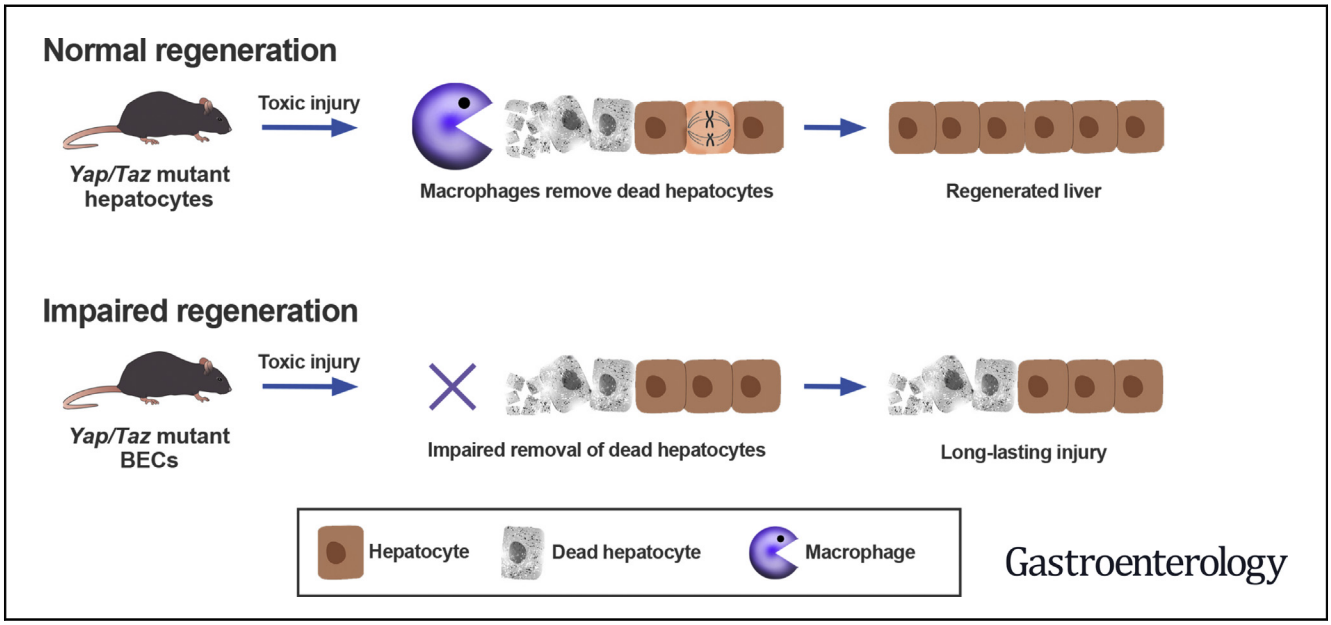

BACKGROUND AND AIMS: The Hippo pathway and its downstream effectors YAP and TAZ (YAP/TAZ) are heralded as important regulators of organ growth and regeneration. However, different studies provided contradictory conclusions about their role during regeneration of different organs, ranging from promoting proliferation to inhibiting it. Here we resolve the function of YAP/TAZ during regeneration of the liver, where Hippo's role in growth control has been studied most intensely. **METHODS:** We evaluated liver regeneration after carbon tetrachloride toxic liver injury in mice with conditional deletion of *Yap*/*Taz* in hepatocytes and/or biliary epithelial cells, and measured the behavior of different cell types during regeneration by histology, RNA sequencing, and flow cytometry. **RESULTS:** We found that YAP/TAZ were activated in hepatocytes in response to carbon tetrachloride toxic injury. However, their targeted deletion in adult hepatocytes did not noticeably impair liver regeneration. In contrast, *Yap/Taz* deletion in adult bile ducts caused severe defects and delay in liver regeneration. Mechanistically, we showed that *Yap/Taz* mutant bile ducts degenerated, causing cholestasis, which stalled the recruitment of phagocytic macrophages and the removal of cellular corpses from injury sites. Elevated bile acids activated pregnane X receptor, which was sufficient to recapitulate the phenotype observed in mutant mice. **CONCLUSIONS:** Our data show that YAP/TAZ are practically dispensable in hepatocytes for liver development and regeneration. Rather, YAP/TAZ play an indirect role in liver regeneration by preserving bile duct integrity and securing immune cell recruitment and function.

Keywords: Hippo Pathway; Toxic Injury; Cholangiocytes; Biliary Epithelial Cells.

WHAT YOU NEED TO KNOW

BACKGROUND AND CONTEXT

The Hippo pathway and its effectors YAP and TAZ are heralded as important regulators of organ growth and regeneration. However, the role of YAP and TAZ in liver regeneration is not resolved.

NEW FINDINGS

Contrary to current belief, we found that YAP and TAZ are not required for the proliferation of hepatocytes during liver regeneration. Rather, loss of YAP and TAZ in biliary epithelial cells caused bile duct deterioration, which secondarily impaired liver regeneration.

LIMITATIONS

This study was performed in the mouse. Further studies are required to determine whether YAP and TAZ function similarly during human liver regeneration.

IMPACT

Our study identifies the function of a main growth control pathway, the Hippo pathway, during liver regeneration, and corrects a widely misconceived importance for this pathway in driving the regenerative proliferation of hepatocytes.

The liver has a remarkable capacity to regenerate, which can be impaired by age and disease. Understanding mechanisms that impair liver regeneration can ultimately enable us to develop new therapies that prompt the liver, and possibly other organs, to regain and enhance their ability to regenerate.

The Hippo pathway is heralded as a key regulator of organ growth and regeneration.[1] Its downstream effectors, the transcriptional co-activators YAP and its homolog TAZ, associate with TEA domain transcription factors (TEAD1–4) to induce the expression of target genes that drive cell proliferation and organ growth.[1] Experimental hyperactivation of YAP/TAZ by their overexpression or by deletion of the upstream negative regulators MST1/2 or the LATS1/2 can trigger overgrowth of many organs in mice.[1] In contrast to these effects, however, deletion of *Yap/Taz* often has little impact on organ growth. In the liver, for example, experimental hyperactivation of YAP triggered hepatocyte hyperproliferation and dramatic liver overgrowth,[1] but conditional deletion of *Yap* (and *Taz*) during embryonic liver development did not impair hepatocyte proliferation and liver growth.[2,3] Notably, YAP/TAZ are the central transducers of the Hippo pathway because deletion of *Yap/Taz* suppressed the tissue overgrowths caused by deletion of the *Mst1/2* or *Lats1/2* kinases.[3–6] The lack of growth defects in *Yap/Taz* mutants is not due to incomplete abolition of Hippo output. Therefore, although excessive YAP/TAZ activity can drive overgrowth, Hippo output is not required for normal growth.

In contrast to embryonic development, it appears that YAP/TAZ are essential for regeneration in different organs, where they can play an instructive role in driving regenerative cell proliferation.[1] In the liver, YAP is transiently activated in hepatocytes upon different types of liver injury,[2,7–13] and experimental hyperactivation of YAP/TAZ in hepatocytes improved liver regrowth after partial hepatectomy.[14,15] Conversely, liver-specific deletion of *Yap* (and *Taz*) reduced and/or delayed regenerative cell proliferation of hepatocytes after different types of liver damage, such as that caused by partial hepatectomy, toxic liver injury, and bile duct ligation (BDL).[2,7–9,16–18] However, the severity of the observed regeneration defects was highly inconsistent between different studies, ranging from no obvious effects to delayed regeneration. These ambiguous results might be explained by the different knockout methods employed. For example, embryonic deletion of *Yap/Taz* with the liver-specific *Alb-Cre* driver resulted in strong regeneration delays,[2] but weaker phenotypes were reported when *Yap* was deleted in adult hepatocytes by hepatocyte-specific small interfering RNAs or by AAV8-Cre, which specifically transduces hepatocytes.[9,16] Notably, *Alb-Cre* starts to be active in embryonic liver precursor cells, the hepatoblasts, which give rise to hepatocytes and biliary epithelial cells (BECs).[19] Therefore, the regeneration defects in *Alb-Cre Yap/Taz* mice could be caused by primary defects during liver development and/or in mature hepatocytes or BECs. In addition, YAP and TAZ can functionally compensate for each other, which could explain weaker phenotypes in single mutants. Because of this, the functions of YAP/TAZ in different liver cell types during hepatocyte regeneration remain unresolved. However, the role of YAP/TAZ for the regeneration of bile ducts is well established. YAP is cell autonomously required in BECs for their proliferative expansion and in hepatocytes for their reprogramming towards a BEC-like fate during a ductular reaction.[7,12,13] Altogether, it is not resolved how YAP/TAZ contributes to liver regeneration.

Material and Methods

A detailed description of the Material and Methods can be found in the Supplementary Material.

Mouse Strains

Albumin-Cre;Yap$^{flox/flox}$;Taz$^{flox/flox}$ mice, *Osteopontin-iCreER^{T2};Yap$^{flox/flox}$;Taz$^{flox/flox}$* mice and *tdTomato* reporter lines were generated by crossing *Yap$^{flox/flox}$;Taz$^{flox/flox}$* (generated by Erik Olson) or *Rosa26-loxP-STOP-loxP-tdTomato (R26-LSL-tdTom)* mice to *Alb-Cre* and *Opn-iCreER^{T2}* mice. *C57Bl/6* mice were from Charles River. Mouse experiments, housing, and

Abbreviations used in this paper: **BDL, bile duct ligation; BEC, biliary epithelial cell; cCasp3, cleaved caspase 3; CCl_4, carbon tetrachloride; FXR, Farnesoid X receptor; KC, Kupffer cell; MDM, monocyte-derived macrophage; PXR, pregnane X receptor; TBlue, Trypan Blue.**

Most current article

0016-5085
https://doi.org/10.1053/j.gastro.2020.10.035

feeding conditions were approved by the Institutional Ethical Commission for Animal Research at Katholieke Universiteit Leuven.

Allele Deletion

Tamoxifen (Sanbio, catalog no. 13258) was intraperitoneally injected on 5 consecutive days (1.6 mg/kg in oil), followed by a 3-week washout period. AAV8 expressing Cre recombinase under a hepatocyte-specific promoter (AAV8.TBG.PI.Cre.rBG; UPenn AV-8-PV1091) was injected intravenously (5×10^{11} gene copies in phosphate-buffered saline).

Immunofluorescent Staining

Livers were embedded in 4% agarose and sectioned using a Vibratome (100 μm). Sections were permeabilized in 0.5% TritonX-100, blocked in 3% bovine serum albumin, and incubated in primary antibodies overnight (Supplementary Table 1). After incubation in secondary antibodies and 4′,6-diamidino-2-phenylindole, sections were mounted and analyzed by confocal microscopy. Images were processed in ImageJ software with Bio-Formats Importer plug-in.

Dead Cell Marking

Dead cells were detected by IgG fluorescent staining on liver sections[20] by 2-hour incubation with AlexaFluor 488 or AlexaFluor 647 donkey-anti-mouse antibodies (Supplementary Table 1). To mark dead cells in vivo, 100 μL of a 0.16% Trypan Blue (TBlue) solution was intravenously injected and analyzed by confocal microscopy.

Quantifications and Statistics

Injury area was quantified using ImageJ software by counting pixels with IgG or TBlue signals per total area, and cleaved Caspase 3 (cCasp3) pixels were counted per IgG pixels. For quantifications of Ki67$^+$, cytokeratin 19$^+$, or tdTomato$^+$ cells, 3 sections per mouse and at least 3 mice were analyzed using ImageJ Cell Counter plugin. Statistical analyses (Student *t* test or Mann-Whitney U test) were performed using Prism8 software (GraphPad) and presented as mean ± SEM after determining normality by Shapiro-Wilk test. A P value of .05 was considered statistically significant (*$P < .05$, **$P < .01$, ***$P < .001$, and ****$P < .0001$).

Results

YAP and TAZ Are Activated in Hepatocytes in Response to Toxic Liver Injury

In the noninjured liver, YAP is expressed in BECs and endothelial cells, but is barely detectable in hepatocytes (Figure 1*A*; Supplementary Figure 1).[3,5] However, YAP accumulated in hepatocyte nuclei after acute liver injury caused by a single injection of the liver toxin carbon tetrachloride (CCl_4) (Figure 1*A*). CCl_4 specifically kills pericentral hepatocytes because they express Cyp2e1, which is required to metabolize CCl_4 into a toxic product (Supplementary Figures 2 and 3).[21] We visualized the area of necrotic hepatocytes by staining with anti-mouse IgG secondary antibodies[21] and YAP was activated in living hepatocytes surrounding the injured areas (Figure 1*A*). YAP levels peaked at 24 hours after injury, and YAP levels or localization did not change in BECs and endothelial cells (Figure 1*B*; Supplementary Figure 4). YAP and TAZ levels were regulated through transcriptional and post-translational mechanisms because regenerating livers had increased levels of *Yap* and *Taz* messenger RNA at 8 hours after injury (Figure 1*C*), and reduced levels of phosphorylated and inactive YAP at 24 hours after CCl_4 injection (Figure 1*B*). Gene expression profiling of purified hepatocytes by RNA sequencing further showed that regenerating hepatocytes at 48 hours after CCl_4 administration up-regulated a set of genes that was highly enriched for a YAP/TAZ target gene signature (Figure 1*D* and *E*). Correspondingly, quantitative reverse transcription polymerase chain reaction of whole liver extracts confirmed an up-regulation of canonical YAP/TAZ target genes and progenitor cell markers in regenerating livers compared with normal livers (Figure 1*F–I*). Thus, YAP/TAZ were activated in hepatocytes in response to toxic liver injury.

Yap and Taz Are Required for Liver Regeneration

To investigate the role of YAP/TAZ during liver regeneration, we deleted *Yap* and *Taz* in embryonic hepatoblasts, the precursor cells for hepatocytes and BECs, using *Alb-Cre*[19] (Supplementary Figure 5*A* and *B*). The livers of adult *Alb-Cre;Yap$^{fl/fl}$;Taz$^{fl/fl}$* mice (hereafter referred to as *Yap/Taz$^{Embr\text{-}KO}$*) had efficiently depleted YAP and TAZ, but had a normal size with normal hepatocyte density and proliferation (Supplementary Figure 5*C–K*). They also had normal liver zonation, revealed by glutamine synthetase and Cyp2e1 expression, in contrast to previous reports (Supplementary Figures 2 and 5*F–K*).[4,22] However, *Yap/Taz$^{Embr\text{-}KO}$* livers had only few and largely disorganized bile ducts, similar but stronger than the phenotype of *Yap* only knockout (Supplementary Figures 5*L* and 6).[3] Mutant mice also had elevated serum levels of alanine aminotransferase, indicating hepatocyte damage (Supplementary Figure 5*M*). Thus, YAP/TAZ are dispensable for embryonic hepatocyte proliferation and liver growth, but are essential for bile duct development, as noted previously.[3]

We then injected adult *Yap/Taz$^{Embr\text{-}KO}$* mice with CCl_4 (Supplementary Figure 7*A*). Their initial area of injury was the same as in wild-type mice 24 hours after CCl_4 injection (Figure 2*A* and *B*). However, injury was still present in *Yap/Taz$^{Embr\text{-}KO}$* mice 96 hours after CCl_4 injection, when wild-type animals had largely restored their liver architecture (Figure 2*A* and *B*). The areas of injury in *Yap/Taz$^{Embr\text{-}KO}$* livers presented many dead hepatocytes that were positive for the cell death marker cCasp3, which was barely detected in wild-type controls (Figure 2*A* and *C* and Supplementary Figure 7*B*). In addition, fewer hepatocytes proliferated in *Yap/Taz$^{Embr\text{-}KO}$* mice compared with controls, although the timing of cell cycle re-entry and exit was similar (Supplementary Figure 7*C* and *D*). Thus, proliferation started at 24 hours after CCl_4 injection and returned back to baseline at 96 hours, but only 22% of the living hepatocytes in *Yap/Taz$^{Embr\text{-}KO}$* mice were positive for the proliferation marker

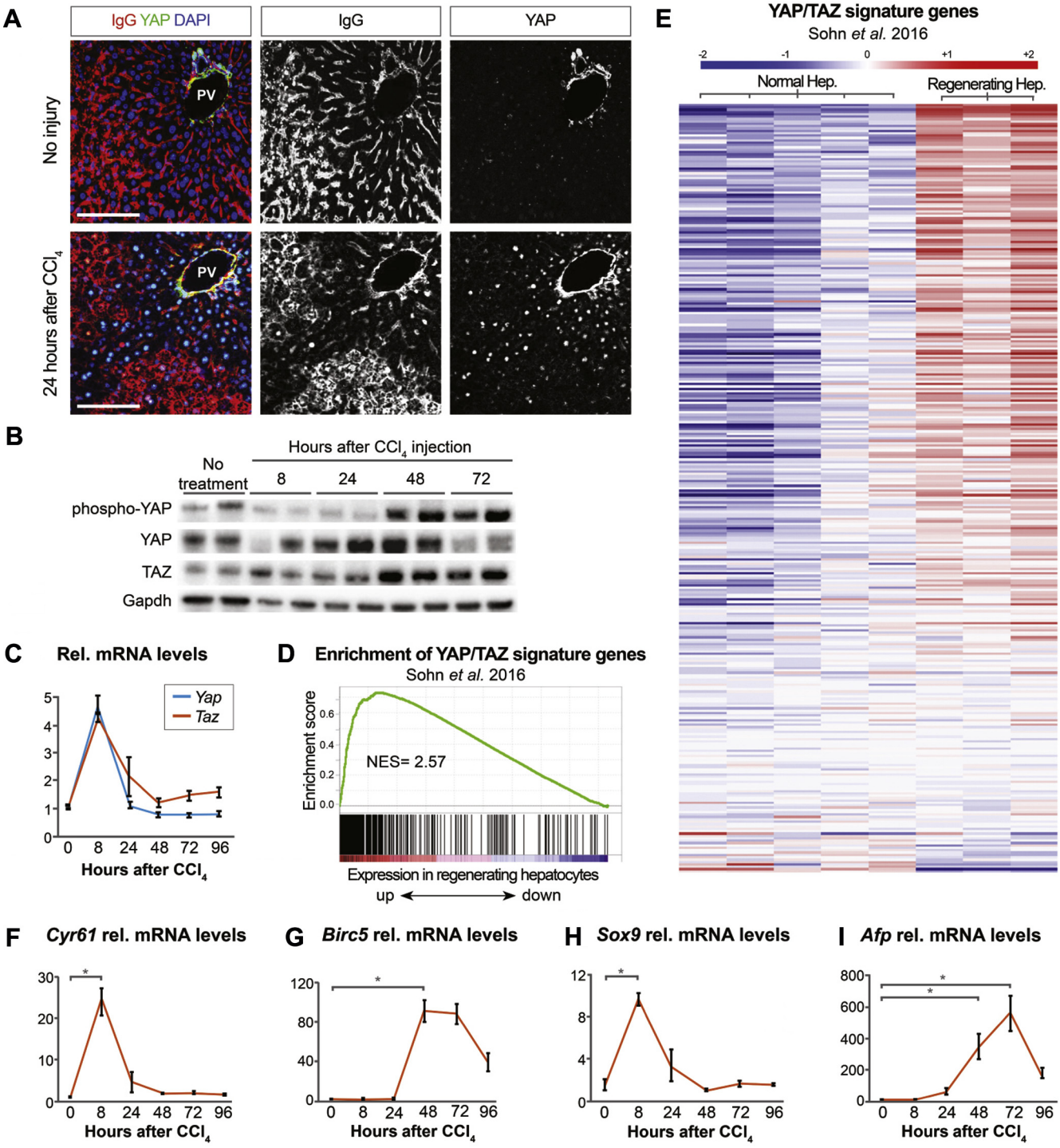

Figure 1. YAP/TAZ are activated in hepatocytes after toxic injury. (*A*) Immunofluorescent detection of YAP on healthy and injured mouse liver sections. Injured areas were marked by mouse IgG (which also marks endothelial cells) and nuclei by 4′,6-diamidino-2-phenylindole (DAPI). *Scale bars:* 100 μm. PV, portal vein. (*B*) Phospho-YAP (Ser-112), total YAP, TAZ, and Gapdh proteins detected by Western blot on normal and regenerating livers. (*C*) *Yap* and *Taz* expression levels in regenerating livers by quantitative reverse transcription polymerase chain reaction (qPCR). n = 3–6. (*D*) *Gene set enrichment analysis plot* showing YAP/TAZ target gene distribution in regenerating hepatocytes (48 hours after CCl_4) relative to normal hepatocytes. Up-regulated genes are ranked on the *left* and down-regulated genes on the *right*. (*E*) *Heatmap* showing up-regulation of YAP/TAZ signature genes in regenerating hepatocytes (48 hours after CCl_4) relative to normal hepatocytes. (*F–I*) *Cyr61, Birc5, Sox9*, and α-*fetoprotein* (*Afp*) expression levels in regenerating livers by qPCR. n = 3–5. mRNA, messenger RNA.

Ki67 at the peak of proliferation, and in wild-type mice this was 52% (Supplementary Figure 7*C* and *D*). Nevertheless, *Yap/Taz* mutants eventually restored normal tissue architecture after 192 hours (Supplementary Figure 7*B*). Thus, embryonic deletion of *Yap/Taz* in hepatoblasts did not prevent liver regeneration, but doubled its length.

Yap and Taz Are Required in Biliary Epithelial Cells But Not Hepatocytes for Liver Regeneration

Because YAP/TAZ are activated in regenerating hepatocytes and are already active in BECs during normal homeostasis, we separately determined their function in adult hepatocytes and BECs during liver regeneration. First, we conditionally deleted *Yap* and *Taz* from adult hepatocytes using an AAV8 that expresses Cre under a hepatocyte-specific promoter (hereafter called AAV-Cre). AAV-Cre was exquisitely efficient and specific for hepatocytes and triggered tdTomato expression from the *R26-LoxP-STOP-LoxP-tdTomato (R26-LSL-tdTom)* reporter transgene in 99.8% of hepatocytes without labeling any BECs (Supplementary Figure 8*A* and *B*). AAV-Cre injection into adult $Yap^{fl/fl}Taz^{fl/fl}$ mice (hereafter referred to as $Yap/Taz^{Hep\text{-}KO}$) strongly reduced *Yap* and *Taz* messenger RNA levels in hepatocytes 3 weeks after knockout (Supplementary Figure 8*C* and *D*). $Yap/Taz^{Hep\text{-}KO}$ mutant mice had normal liver morphology, zonation, and function (Supplementary Figure 8*E–H*). Surprisingly, they also properly regenerated liver injuries caused by CCl_4 and partial hepatectomy with normal levels of hepatocyte proliferation (Figure 2 and Supplementary Figures 9 and 10).

We then deleted *Yap* and *Taz* from BECs in adult mice using the inducible *Osteopontin-iCreER*^{T2} (*Opn-iCreER*^{T2}) driver. *Opn-iCreER*^{T2} triggered tdTomato expression from the *R26-LSL-tdTom* reporter in 100% of cytokeratin 19 expressing BECs, but in virtually no hepatocytes after 5 days of tamoxifen injections (Supplementary Figure 11*A*).[23] Tamoxifen injections into $Opn\text{-}iCreER^{T2};Yap^{fl/fl}Taz^{fl/fl}$ mice (hereafter called $Yap/Taz^{BEC\text{-}KO}$) resulted in robust reduction of YAP and TAZ protein levels in BECs 3 weeks after the start of tamoxifen injections (Supplementary Figure 11*B*). Such $Yap/Taz^{BEC\text{-}KO}$ mice had strong liver regeneration defects; they had lingering injury beyond 96 hours after CCl_4 injection, drastically elevated levels of cCasp3-positive cells throughout regeneration, and reduced hepatocyte proliferation, despite unaltered YAP/TAZ expression in hepatocytes (Figure 2 and Supplementary Figure 12). Consequently, $Yap/Taz^{BEC\text{-}KO}$ mice only recovered after 192 hours, which is twice as long as control and $Yap/Taz^{Hep\text{-}KO}$ mice (Supplementary Figure 12*B*). Deletion of *Yap/Taz* in adult BECs thus phenocopied the regeneration defects observed in $Yap/Taz^{Embr\text{-}KO}$ mice.

Yap and Taz Are Required to Maintain Bile Duct Integrity and Function

To understand how deletion of *Yap/Taz* in bile ducts affects liver regeneration, we first analyzed effects on bile duct morphology and function. Visualization of the biliary tree by injecting china ink into the common bile duct revealed that the biliary trees of $Yap/Taz^{BEC\text{-}KO}$ and $Yap/Taz^{Embr\text{-}KO}$ livers were truncated and less ramified than normal, and mainly comprised large bile ducts (Figure 3*A*). Removing *Yap/Taz* from adult hepatocytes in addition to BECs did not modify the phenotype (Supplementary Figure 13). We then quantified the percentage of portal areas containing bile ducts, identifying portal veins by the absence of glutamine synthetase expression when no bile ducts were present. While in wild-type livers, nearly all portal areas had at least 1 bile duct, <40% of portal areas had bile ducts in *Yap/Taz* mutants (Figure 3*B* and *C*). Furthermore, the remaining bile ducts in $Yap/Taz^{BEC\text{-}KO}$ livers showed severe morphologic defects; they had collapsed lumens, mislocalization of the apical protein osteopontin, and decreased numbers of BECs per duct (Figure 3*D* and *E*). Mutant BECs did not completely lose cell polarity because other cell polarity markers, such as atypical protein kinase C, E-cadherin, β-catenin, Claudin-3, and the Golgi apparatus, localized properly (Figure 3*E* and Supplementary Figure 14). Thus, deletion of *Yap/Taz* in adult BECs caused a morphologic disorganization and loss of BECs and bile ducts.

Defective bile ducts can result in cholestasis.[24] Indeed, mutant mice had elevated levels of bile acids in the serum, which was more severe in $Yap/Taz^{Embr\text{-}KO}$ mice than in $Yap/Taz^{BEC\text{-}KO}$ mice, reflecting their stronger phenotype (Figure 3*F*). Mutant mice had further characteristics of cholestasis; they had high levels of circulating alanine aminotransferase indicating hepatocyte injury, although without obvious morphologic defects in hepatocytes (Figure 3*G*), and their periportal hepatocytes down-regulated the bile acid transporters Bsep and Mrp-2 (Supplementary Figure 15*A* and *B*), which is an adaptive response to cholestatic injury that limits canalicular but promotes basolateral secretion of bile acids into the blood stream.[25,26] Furthermore, hepatocytes of mutant mice up-regulated a cholestatic gene expression profile (Supplementary Figure 16)[27,28] and down-regulated the expression of the canalicular cell adhesion molecule Ceacam-1 (Supplementary Figure 15*C*), as previously reported after bile acid overload.[29] Altogether, these data show that loss of *Yap/Taz* in adult BECs causes bile duct defects and cholestasis.

Cholestasis Recapitulates Liver Regeneration Defects of $Yap/Taz^{BEC\text{-}KO}$ *Mice*

To test whether elevated bile acids are sufficient to mimic the regeneration defects of $Yap/Taz^{BEC\text{-}KO}$ mutant mice, we induced cholestasis by BDL in wild-type mice. As expected, BDL caused acute cholestasis with highly increased levels of bile acids and alanine aminotransferase in the blood serum, formation of bile lakes in the liver parenchyma, and down-regulation of Bsep and Mrp-2 (Supplementary Figure 15). We then injected CCl_4 at 48 hours after BDL and monitored liver regeneration (Figure 4*A*). These mice had defects in liver regeneration similar to $Yap/Taz^{BEC\text{-}KO}$ and $Yap/Taz^{Embr\text{-}KO}$ mutant mice. They showed delayed regeneration with persisting areas of necrotic hepatocytes, they had many cCasp3-positive cells in

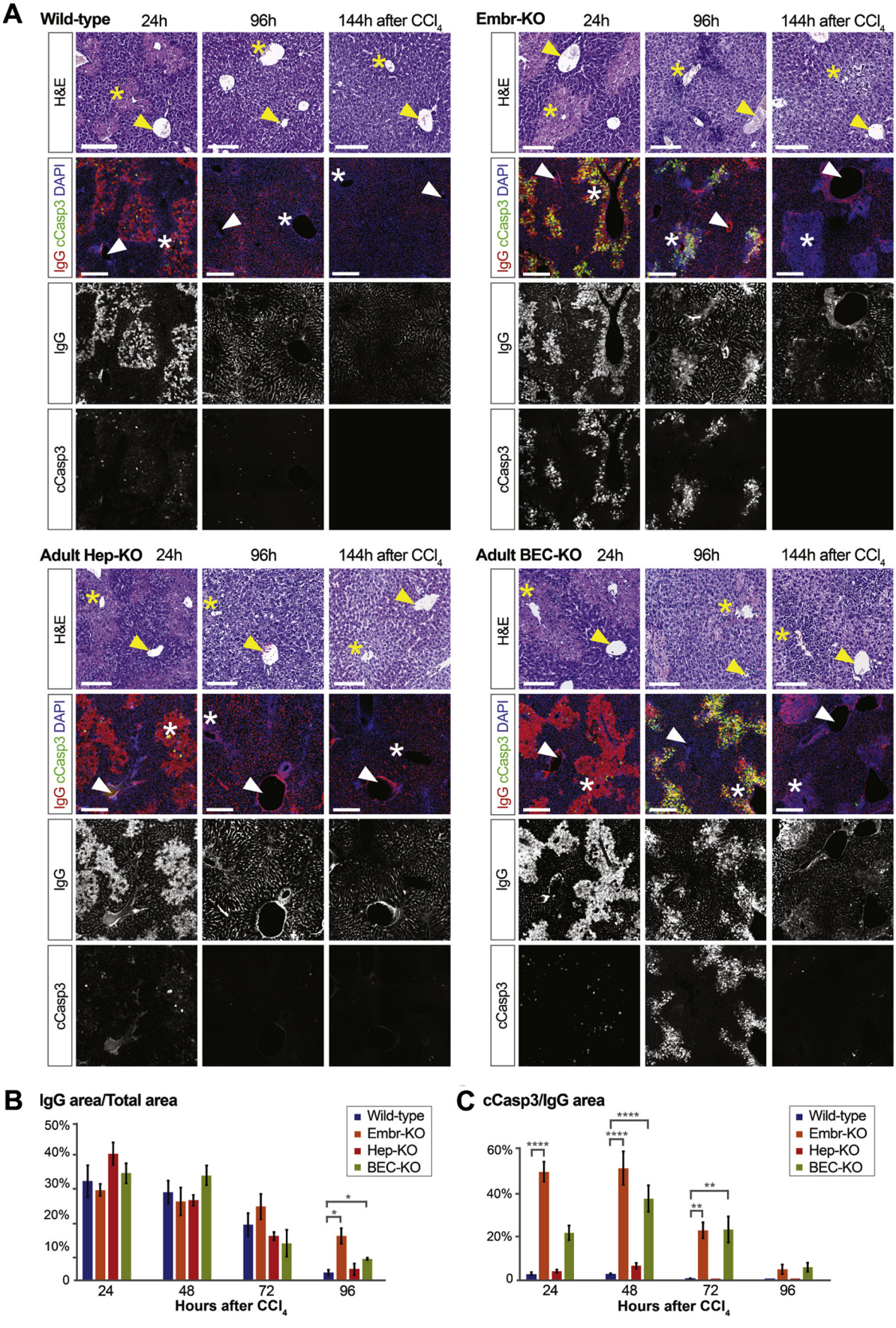
A
Wild-type
24h
96h
144h after CCl4
Embr-KO
Adult Hep-KO
Adult BEC-KO
H&E
IgG cCasp3 DAPI
IgG
cCasp3
B
IgG area/Total area
50%
40%
30%
20%
10%
0
24
48
72
96
Hours after CCl4
Wild-type
Embr-KO
Hep-KO
BEC-KO
C
cCasp3/IgG area
60%
40%
20%
0
****
**
*

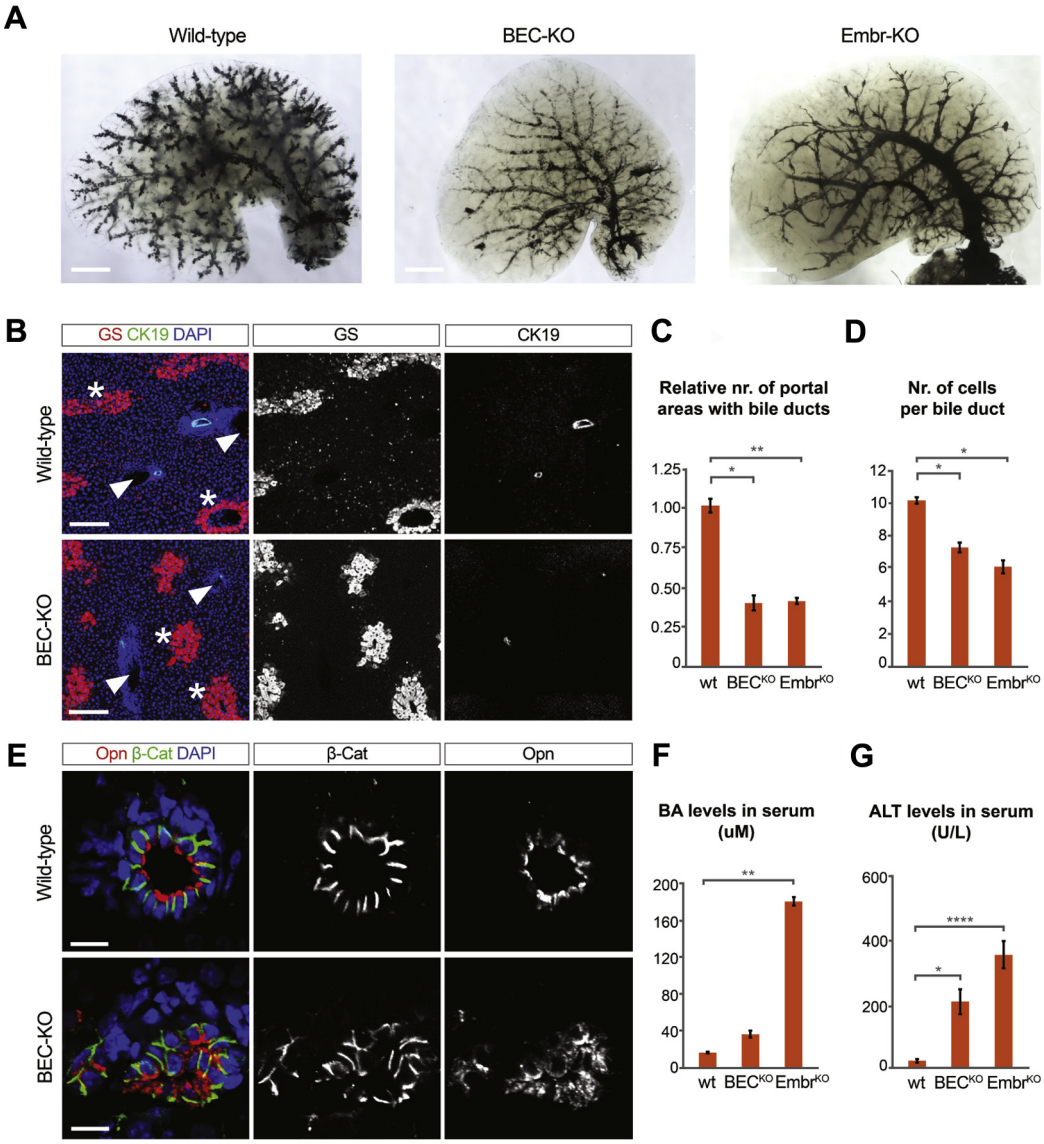

Figure 3. Loss of YAP and TAZ in BECs impairs bile duct integrity and causes cholestasis. (*A*) Caudate liver lobes from wild-type and *Yap/Taz* knockout livers showing the biliary tree after retrograde ink injection into the common bile duct. *Scale bars:* 1 mm. (*B*) Immunofluorescent detection of cytokeratin 19 (CK19) and glutamine synthetase (GS) on liver sections from wild-type and *Yap/Taz*$^{BEC\text{-}KO}$ mice. *Scale bars:* 200 μm. *Asterisks:* central veins. *Arrowheads:* portal veins. (*C*) Relative number of portal regions containing lumenized bile ducts expressing CK19 and (*D*) absolute number of CK19-expressing cells per bile duct in wild-type and knockout mice. n = 4. (*E*) Immunofluorescent detection of osteopontin (Opn) and β-Catenin (β-Cat) on bile ducts in liver sections from wild-type and *Yap/Taz*$^{BEC\text{-}KO}$ mice. *Scale bars:* 10 μm. (*F*, *G*) Serum levels of bile acids (BAs) and alanine aminotransferase (ALT) at 8 weeks of age (*Yap/Taz*$^{Embr\text{-}KO}$ mice) or 3 weeks after tamoxifen (*Yap/Taz*$^{BEC\text{-}KO}$ mice). n $\geq$ 5. DAPI, 4′,6-diamidino-2-phenylindole.

injured areas, and they had fewer proliferating hepatocytes compared with CCl_4-treated, sham-operated mice, which regenerated normally (Figure 4*B*–*F*). These results support the hypothesis that cholestasis causes the liver regeneration defects in mice with *Yap/Taz* mutant bile ducts.

Clearance of Necrotic Hepatocytes Is Impaired in Yap/Taz$^{BEC\text{-}KO}$ *Mutant Mice*

To understand the mechanisms of liver regeneration defects in *Yap/Taz*$^{BEC\text{-}KO}$ mutant mice, we investigated their most conspicuous phenotype, namely, the persistence of

Figure 2. *Yap/Taz* deletion in bile ducts causes liver regeneration defects. (*A*) H&E staining and immunofluorescent detection of dead cells by IgG or cCasp3 staining in wild-type and *Alb-Cre;Yap*$^{fl/fl}$;*Taz*$^{fl/fl}$(Embr-KO), *Yap*$^{fl/fl}$;*Taz*$^{fl/fl}$ plus AAV-Cre (Hep-KO) and *Opn-CreER*^{T2};*Yap*$^{fl/fl}$;*Taz*$^{fl/fl}$ plus tamoxifen (BEC-KO) after CCl_4. *Scale bars:* 200 μm. *Asterisks:* central veins. *Arrowheads:* portal veins. (*B*) Quantification of total injury area (IgG staining) or (*C*) of apoptosis (cCasp3 staining) in livers treated with CCl_4. n = 3–4. DAPI, 4′,6-diamidino-2-phenylindole.

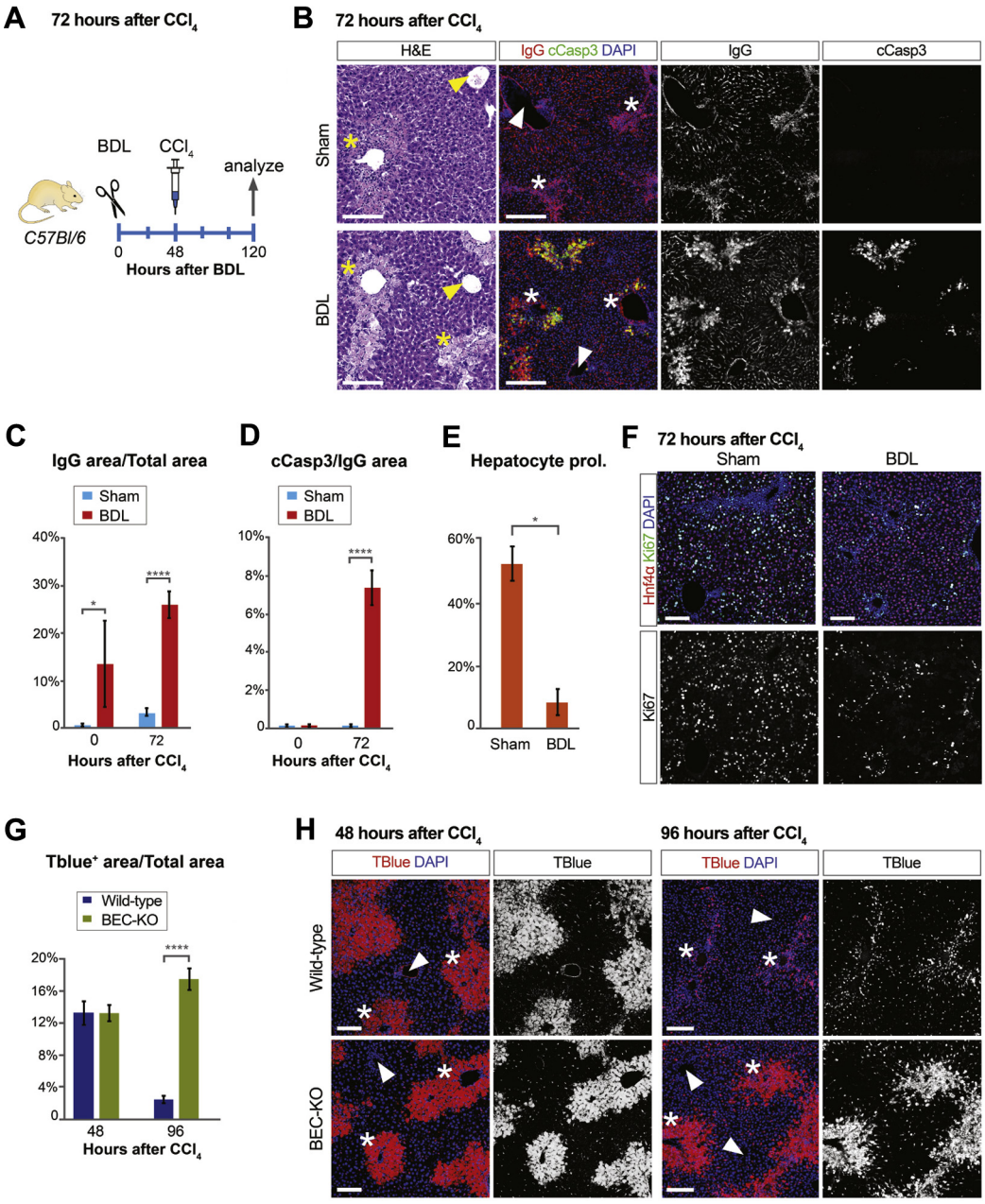

Figure 4. Cholestasis impairs liver regeneration after toxic liver injury by inhibiting the removal of dead cell bodies. (*A*) Schematic experimental outline. Eight-week-old *C57Bl/6* mice subjected to BDL were injected with CCl_4 at 48 hours after BDL. Mice were sacrificed at 72 hours after CCl_4 administration. (*B*) H&E staining and immunofluorescent detection of IgG and cCasp3 in livers from sham and BDL mice at 72 hours after CCl_4 treatment. *Scale bars:* 200 μm. (*C*, *D*) Quantification of liver injury area stained by IgG and cCasp3. n $\geq$ 4. (*E*, *F*) Quantification and immunofluorescent staining of Ki67 and Hnf4α expression in proliferating hepatocytes from sham and BDL livers. *Scale bars:* 100 μm. n = 4. (*G*) Quantification of injury area (TBlue) after CCl_4 treatment. TBlue was administered at 24 hours after CCl_4 injection. n $\geq$ 5. (*H*) In vivo tracing of injured liver area by TBlue administered at 24 hours after CCl_4 injection. *Scale bars:* 100 μm. *Asterisks:* central veins. *Arrowheads:* portal veins. DAPI, 4′,6-diamidino-2-phenylindole.

large areas of dead hepatocytes. This could be a consequence of impaired removal of dead hepatocytes or because hepatocytes were continuously dying. To distinguish between these 2 possibilities, we performed a pulse-chase experiment to monitor the dynamics of hepatocyte death. We labeled dying cell corpses in vivo by TBlue injection after CCl_4 injection, and then quantified the number of $TBlue^+$ cells still present at later time points. Importantly, a control experiment showed that TBlue effectively labeled dying hepatocytes that were present at the time of TBlue injection, but none of those that were killed 24 hours after TBlue injection or later (Supplementary Figure 17*A*). Therefore, TBlue circulation was short-lived and this method can be used to track dead cells. TBlue also stained

living immune and endothelial cells for unknown reasons (Supplementary Figure 18), but these cells could easily be recognized by their size and location and were excluded. We then injected TBlue 24 hours after CCl_4 injection and analyzed mice at later time points. Forty-eight hours after CCl_4, wild-type and *Yap/Taz*$^{BEC\text{-}KO}$ livers contained many IgG$^+$ dead cells, all of which were labeled with TBlue (Figure 4*G* and *H* and Supplementary Figure 17*B*). However, 96 hours after CCl_4, wild-type mice were healed and no longer contained TBlue$^+$ cells, whereas *Yap/Taz*$^{BEC\text{-}KO}$ mutants still had large numbers of TBlue$^+$ cells (Figure 4*G* and *H*). This result indicated that CCl_4 injection induced a single wave of cell death in wild-type and *Yap/Taz*$^{BEC\text{-}KO}$ mutants and that mutant mice had lingering dead cell corpses because they were not removed.

Yap/Taz$^{BEC\text{-}KO}$ *Mutants Have Impaired Macrophage Recruitment and Polarization*

Necrotic cell corpses are mainly removed by macrophages.[30] In wild-type mice, the number of resident macrophages (Kupffer cells [KCs]; F4/80^{hi}CD11b^{int}) declined during the initial phase after CCl_4, but then reappeared and accumulated around the regenerating regions at 72 hours after CCl_4 (Figure 5*A*–*D* and Supplementary Figure 19*A*).[31] This reappearance of KCs was preceded by a dramatic influx of infiltrating monocytes (F4/80^{int}CD11b^{hi}Ly6C^{hi}) at 48 hours after CCl_4 (Figure 5*E* and Supplementary Figure 19*B*), which probably produced at least some of the newly emerging macrophages at 72 hours.[32] In contrast, *Yap/Taz*$^{BEC\text{-}KO}$ mutants had markedly reduced numbers of F4/80$^+$ macrophages in pericentral regions at 72 hours and significantly less infiltrating monocytes compared to wild-type (Figure 5*A*–*E* and Supplementary Figure 19*B*). Only much later, at 144 hours after CCl_4, mutant livers started to accumulate F4/80$^+$ cells in the damaged areas (Figure 5*D* and *F*). Mutant mice presented features of coagulating necrosis, which is characterized by the preservation of dead tissue for days and massive accumulation of macrophages.[33] These defects in monocyte recruitment were recapitulated in wild-type mice after BDL combined with CCl_4, suggesting that they are caused by cholestasis (Figure 5*G*). However, neutrophil numbers were elevated in wild-type and *Yap/Taz*$^{BEC\text{-}KO}$ livers during injury, although mutants had higher background numbers, possibly as a result of cholestasis (Supplementary Figure 19*B* and *C*). We concluded that the immune response was significantly delayed, although not completely halted, in *Yap/Taz*$^{BEC\text{-}KO}$ livers.

In order to determine the importance of these macrophage defects for the mutant phenotypes, we injected clodronate liposomes into wild-type mice, which effectively depleted all macrophages (Supplementary Figure 20*A*–*C*) and then injected CCl_4 24 hours later. Strikingly, macrophage-depleted mice phenocopied the regeneration defects of *Yap/Taz*$^{BEC\text{-}KO}$ mutant livers; they had lingering corpses of necrotic hepatocytes marked by IgG, cCasp3, and TBlue (Figure 6*A*–*C* and Supplementary Figure 20*D* and *E*). These results indicate that defective monocyte recruitment and KC restoration caused the lack of necrotic cell clearance and subsequent regeneration defects in *Yap/Taz*$^{BEC\text{-}KO}$ mutant mice.

We then investigated the polarization of monocyte-derived macrophages (MDMs; F4/80^{int}CD11b^{hi}Ly6C^{neg}) into pro-inflammatory M1-like macrophages and anti-inflammatory M2-like macrophages that also remove necrotic debris and facilitate tissue repair.[34] We found that the numbers of MDMs, as opposed to the effect on F4/80+ KCs, did not differ between wild-type and *Yap/Taz*$^{BEC\text{-}KO}$ mutant livers (Supplementary Figure 19*B*–*D*). However, the number of MDMs with M2 characteristics (high CD206 expression[35]) increased at 72 hours after injury in wild-type mice, but remained unchanged throughout liver regeneration in *Yap/Taz*$^{BEC\text{-}KO}$ mice (Figure 6*D* and *E*). This phenotype was also confirmed by measuring mean fluorescence intensity, which detected lower CD206 expression in mutant mice compared with wild-type at 72 hours after CCl_4 (Figure 6*F*). However, the number of MDMs with M1 characteristics (detected by CD38 high expression[36]) did not change in wild-type and mutant mice during the course of liver regeneration (Supplementary Figure 19*E*–*G*).

Defects in macrophage activation were also detected at the level of gene expression profiles by RNA sequencing of purified macrophages. Before injury, gene expression profiles of macrophages from wild-type and mutant mice were nearly identical. CCl_4 treatment caused up-regulation of 522 genes in macrophages of wild-type livers, but macrophages of *Yap/Taz*$^{BEC\text{-}KO}$ livers only up-regulated 303 of these genes after CCl_4 (Figure 6*G*). Gene ontology terms for these 303 genes were strongly enriched for cell proliferation processes. Interestingly, the remaining 219 genes that were induced in macrophages from wild-type, but not mutant, livers were associated with leukocyte activation and migration (Figure 6*G*). More specifically, genes lacking in macrophages of mutant livers play important roles in chemoattraction of monocytes (*Il7r, Clec4d, Cd11c*), M2 polarization (*Galectin-3, Mmp8, Chil3*), actin remodeling, and phagocytosis (*Atp6v0d2, Slamf7/8, Gpnmb*). Macrophages of *Yap/Taz*$^{BEC\text{-}KO}$ mice only partially responded to toxic injury, as they induced genes involved in cell proliferation but failed to activate genes important for immune cell migration, clearance of cellular debris, and polarization towards restorative macrophages. Our fluorescence-activated cell sorting and RNA sequencing results showed that *Yap/Taz*$^{BEC\text{-}KO}$ mice were compromised in KC restoration and in the activation and polarization of MDMs towards an M2-like, restorative phenotype after CCl_4 injury. Both phenotypes most likely contributed to the lack of necrotic cell clearance and subsequent regeneration defects in *Yap/Taz*$^{BEC\text{-}KO}$ mutant mice.

Pregnane X Receptor Activation Inhibits Immune Cell Activation and Recruitment

We next investigated whether defects in hepatocyte signaling could be responsible for impaired immune cell recruitment and activation. We analyzed the transcriptional profile of regenerating hepatocytes in wild-type and *Yap/Taz*$^{BEC\text{-}KO}$ livers at 48 hours after CCl_4 by RNA

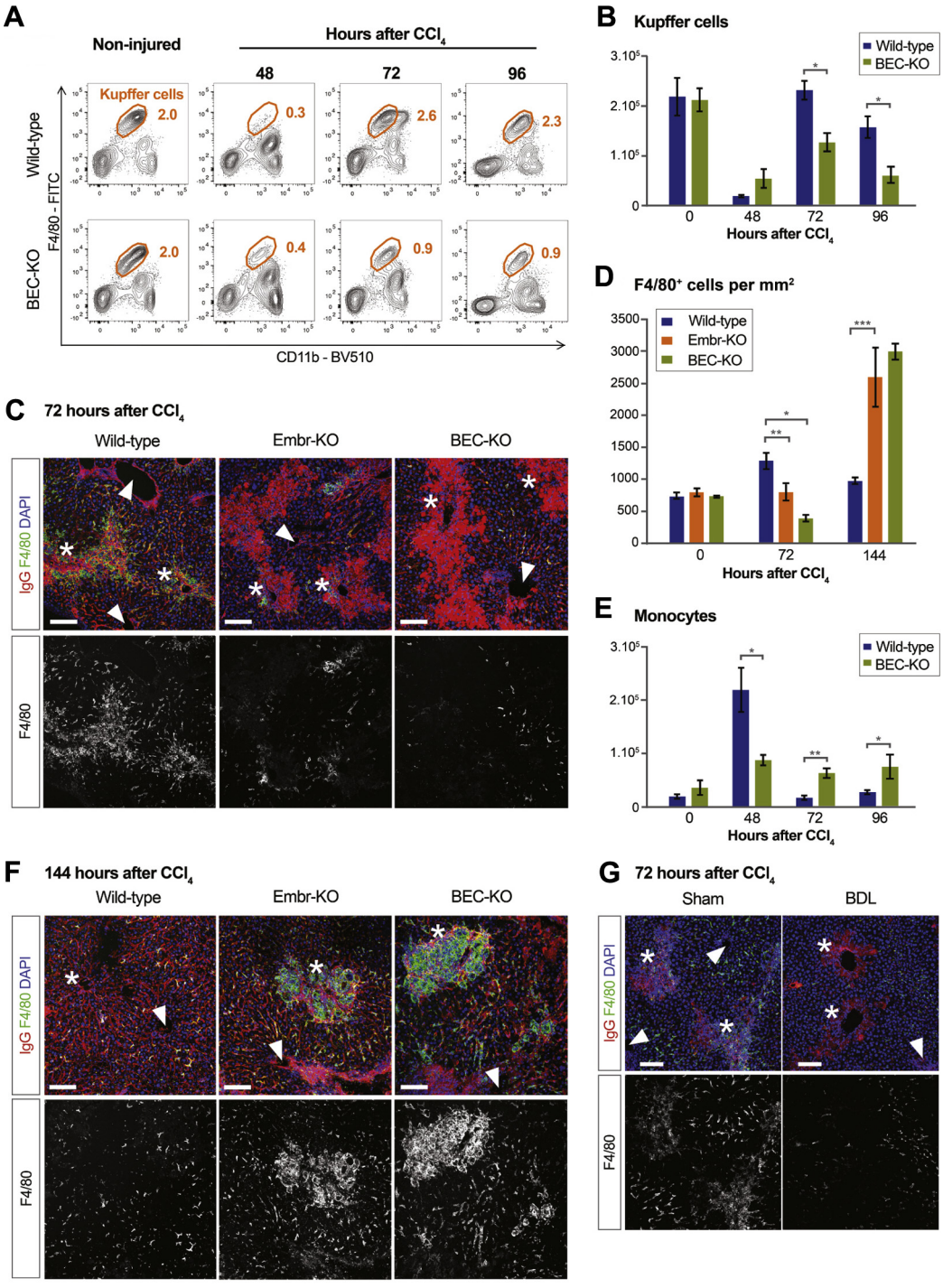

Figure 5. *Yap/Taz*$^{BEC\text{-}KO}$ mutant mice have impaired macrophage recruitment during regeneration. (*A*) Time-course analysis of immune cell kinetics by flow cytometry in injured livers from wild-type and *Yap/Taz*$^{BEC\text{-}KO}$ mice after CCl_4 injection. The absolute number of KCs (F4/80^{hi} CD11b^{int}; in *orange*) in the nonparenchymal fraction (NPF) is expressed in 100,000s. (*B*) Absolute numbers of KCs in the NPF of regenerating wild-type and *Yap/Taz*$^{BEC\text{-}KO}$ livers by flow cytometry. n = 4–6. (*C*) Immunofluorescent detection of F4/80^{+} immune cells at the area of injury (IgG). *Scale bars:* 100 μm. (*D*) Quantification of F4/80^{+} immune cells per unit of area on sections from injured livers. n $\geq$ 4. (*E*) Absolute number of monocytes (F4/80^{int}CD11b^{hi}Ly6C^{hi}) in the NPF of regenerating wild-type and *Yap/Taz*$^{BEC\text{-}KO}$ livers by flow cytometry. n = 4–6. (*F*) Immunofluorescent detection of F4/80^{+} immune cells at area of injury (IgG). *Scale bars:* 100 μm. (*G*) Immunofluorescent detection of IgG and F4/80^{+} cells on sections of BDL-treated mice 72 hours after CCl_4. *Scale bars:* 100 μm. *Asterisks:* central veins; *arrowheads:* portal veins. DAPI, 4′,6-diamidino-2-phenylindole.

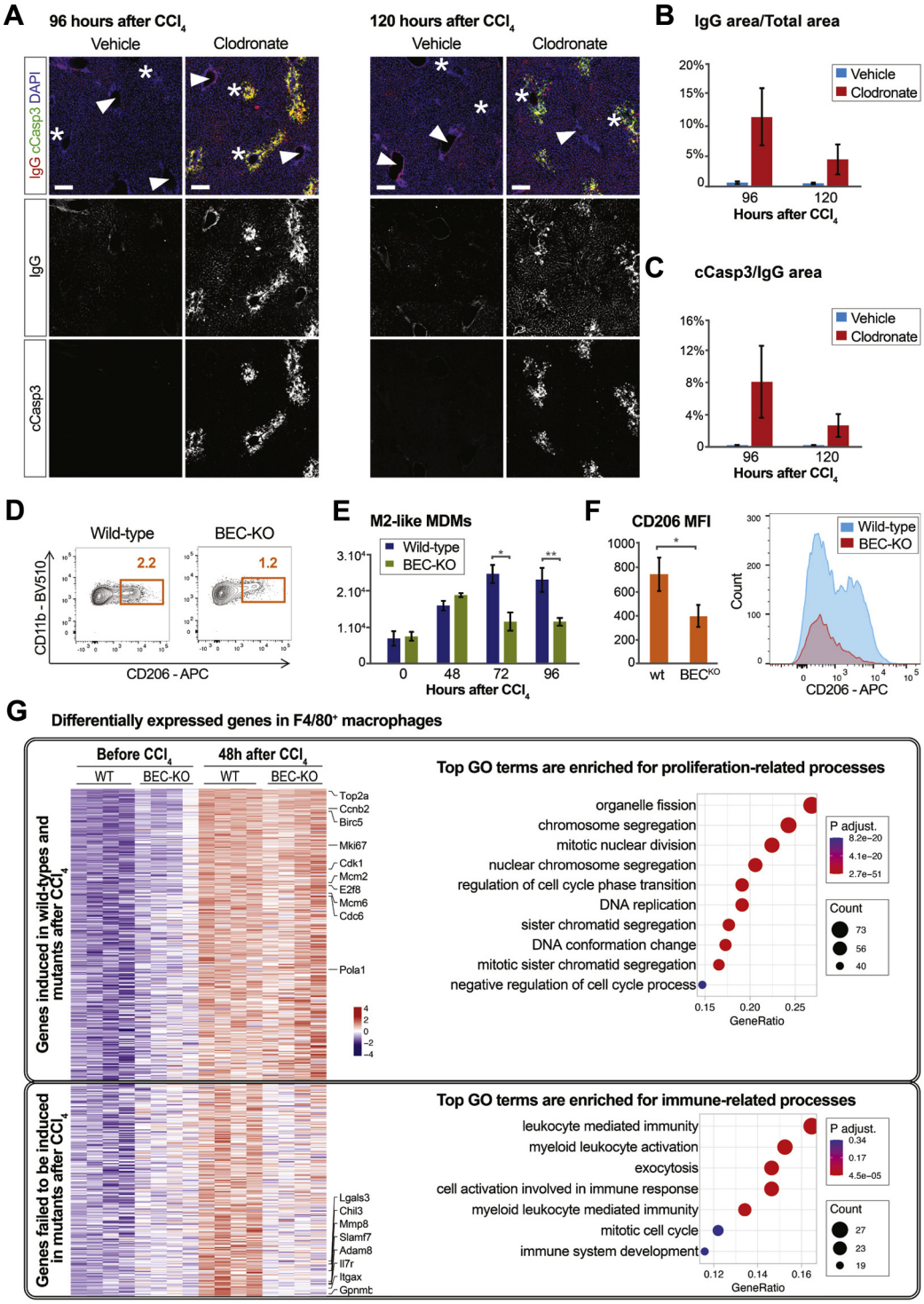

Figure 6. Macrophages of *Yap/Taz*$^{BEC\text{-}KO}$ mutant livers have an aberrant response to liver injury. (*A–C*) Immunofluorescent detection and quantifications of injured liver area (IgG and cCasp3) after CCl_4 in mice treated with vehicle or clodronate liposomes. *Scale bars:* 200 μm. *Asterisks:* central veins. *Arrowheads:* portal veins. n $\geq$ 5. (*D*) Representative flow cytometry *dot plots* of CD206$^+$ M2-like MDMs at 72 hours after CCl_4 in wild-type and *Yap/Taz*$^{BEC\text{-}KO}$ livers. The absolute number of M2-like MDMs (*orange*) in the nonparenchymal fraction (NPF) is expressed in 10,000s. (*E*) Quantification of absolute numbers of CD206$^+$ M2-like MDMs after CCl_4 in the NPF of wild-type and *Yap/Taz*$^{BEC\text{-}KO}$ mice by flow cytometry. n = 4–6. (*F*) Mean fluorescent intensity (MFI) of CD206 expression in MDMs in the liver 72 hours after CCl_4 injection. n = 3. (*G*) *Heatmap* showing normalized expression of 522 genes significantly up-regulated in wild-type macrophages of injured livers (48 hours after CCl_4) relative to macrophages of healthy livers (*left*). *Dot plots* of gene ontology (GO) terms associated with 303 genes significantly up-regulated in macrophages of all injured livers (wild-type and *Yap/Taz*$^{BEC\text{-}KO}$; top right) or 219 genes significantly induced by CCl_4 in macrophages of wild-type livers, but not of *Yap/Taz*$^{BEC\text{-}KO}$ livers (*bottom right*). DAPI, 4′,6-diamidino-2-phenylindole.

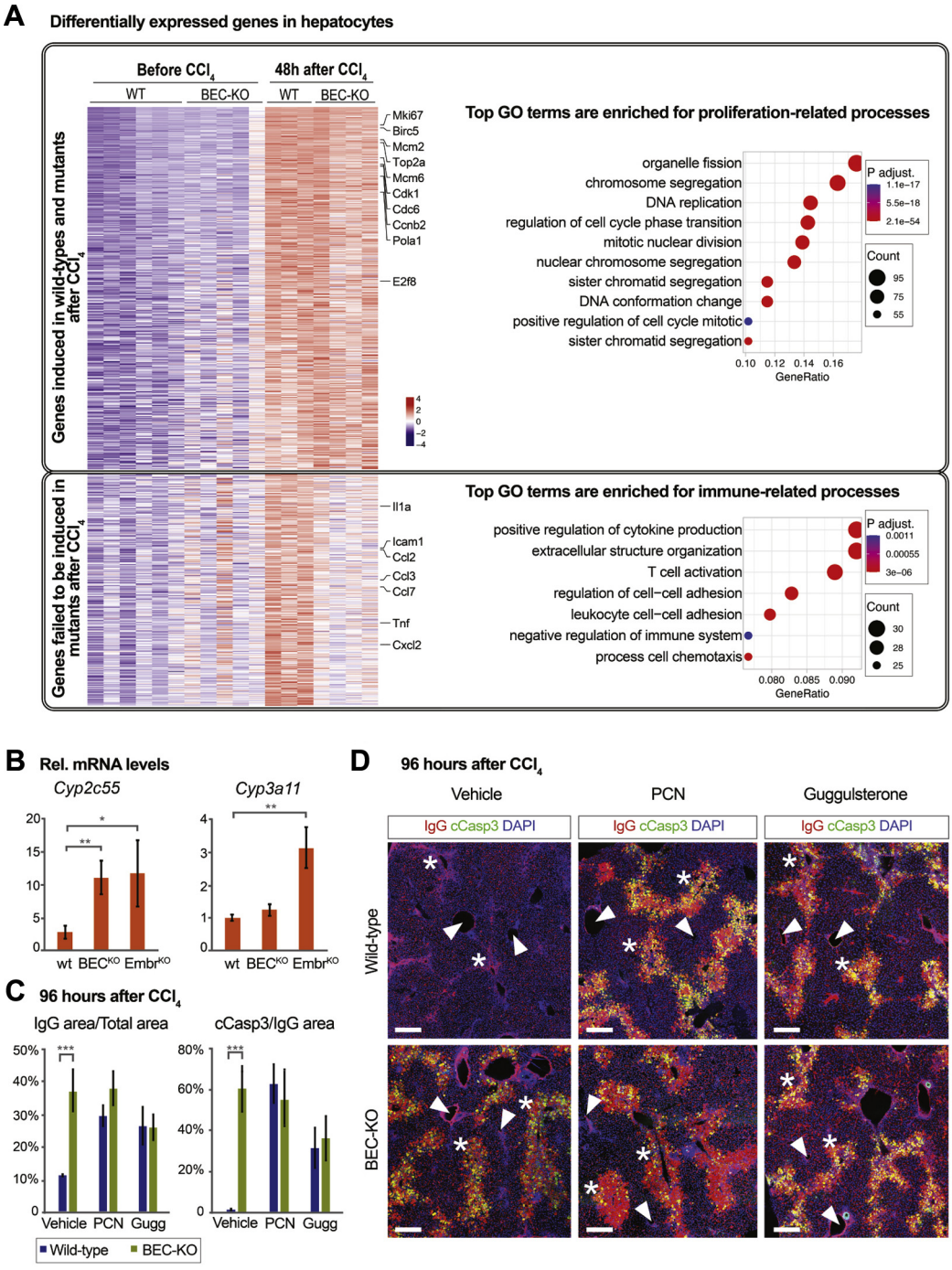

Figure 7. Decreased hepatocyte-derived cytokine expression compromises immune cell recruitment in *Yap/Taz*$^{BEC\text{-}KO}$ mutant livers. (*A*) *Heatmap* showing normalized expression of 1147 genes significantly up-regulated in wild-type (WT) hepatocytes of injured livers (48 hours after CCl_4) relative to hepatocytes of healthy livers (*left*). *Dot plot* of gene ontology (GO) terms associated with 691 genes significantly up-regulated in hepatocytes of all injured livers (WT and *Yap/Taz*$^{BEC\text{-}KO}$; *top right*) or 456 genes significantly induced by CCl_4 in hepatocytes of WT livers, but not of *Yap/Taz*$^{BEC\text{-}KO}$ livers (*bottom right*). (*B*) PXR target gene expression levels in WT and *Yap/Taz*$^{BEC\text{-}KO}$ livers by quantitative reverse transcription polymerase chain reaction. n = 3–6. (*C*, *D*) Immunofluorescent staining and quantification of IgG and cCasp3 on regenerating WT and *Yap/Taz*$^{BEC\text{-}KO}$ livers after pregnenolone-16α-carbonitrile (PCN), Guggulsterone (Gugg) or vehicle treatment. *Scale bars*: 200 μm. *Asterisks*: central veins. *Arrowheads*: portal veins. DAPI, 4′,6-diamidino-2-phenylindole; mRNA, messenger RNA.

sequencing of purified hepatocytes. This analysis identified 1147 genes that were significantly up-regulated after CCl_4 injury in hepatocytes of wild-type mice (Figure 7*A*). In *Yap/Taz*$^{BEC\text{-}KO}$ mutants, 691 of these genes were still induced, although at slightly lower levels, which are strongly enriched for gene ontology terms related to cell proliferation (Figure 7*A*). However, hepatocytes from mutant mice failed to up-regulate the other 456 genes that

are strongly enriched in gene ontology terms related to cytokine and chemokine signaling, including *Ccl2*, which encodes a major monocyte attractant (Figure 7*A*).[37] Hepatocytes of *Yap/Taz*$^{BEC\text{-}KO}$ mice failed to activate genes important for the nonautonomous induction of cell migration and immune cell activation.

Finally, we wanted to unravel the mechanisms by which elevated levels of bile acids cause defects in the response of hepatocytes to liver injury. Bile acids can be directly toxic to liver cells due to their detergent properties, but they can also act as signaling molecules and bind to different receptors, in particular the nuclear hormone receptors Farnesoid X receptor (FXR) and pregnane X receptor (PXR), which are highly expressed in hepatocytes, and TGR5, which is expressed in macrophages.[38] Although TGR5 target genes were not up-regulated in livers of *Yap/Taz*$^{BEC\text{-}KO}$ mice (Supplementary Figure 21), FXR target genes were slightly increased in *Yap/Taz*$^{Embr\text{-}KO}$ and *Yap/Taz*$^{BEC\text{-}KO}$ mice (Supplementary Figure 22). However, the FXR agonist obeticholic acid did not induce regeneration defects in wild-type mice after CCl_4 (Supplementary Figure 22*C* and *D*). In contrast, PXR target genes (*Cyp2c55* and *Cyp3a11*)[39] were strongly up-regulated in *Yap/Taz*$^{Embr\text{-}KO}$ and *Yap/Taz*$^{BEC\text{-}KO}$ mutant mice compared with wild-type (Figure 7*B*), similar to their induction in cholestatic patients.[40] Strikingly, pharmacologic hyperactivation of PXR by treating wild-type mice with the PXR agonist pregnenolone-16α-carbonitrile[39] before CCl_4 injection was sufficient to recapitulate the regeneration defects of *Yap/Taz*$^{BEC\text{-}KO}$ mutant mice, including impaired necrotic cell clearance, high levels of cCasp3, and delayed regeneration (Figure 7*C* and *D*). As expected, pregnenolone-16α-carbonitrile injection caused strong induction of PXR target genes (Supplementary Figure 23*A*). Similarly, treatment of wild-type mice with guggulsterone, which inhibits FXR[41] but activates PXR,[42] phenocopied the regeneration defects observed in *Yap/Taz*$^{BEC\text{-}KO}$ mutant mice after CCl_4 (Figure 7*C* and *D* and Supplementary Figure 23*B*). Because PXR can suppress cytokine expression in hepatocytes, monocytes, and macrophages,[43,44] the regeneration defects of *Yap/Taz*$^{BEC\text{-}KO}$ mice can be explained by the activation of PXR by bile acids in hepatocytes.

Discussion

In this study, we addressed the function of the Hippo pathway in liver regeneration. It is widely thought that the Hippo pathway effectors YAP/TAZ orchestrate liver regeneration and instructively drive hepatocyte proliferation. However, although it is true that mice in which *Yap/Taz* were knocked out in embryonic hepatoblasts have severe defects in liver regeneration, including reduced hepatocyte proliferation, we found that these phenotypes are not the consequence of a lack of YAP/TAZ in hepatocytes but in BECs. Therefore, conditional deletion of *Yap/Taz* in adult BECs phenocopied the embryonic hepatoblast knockout and indirectly suppressed the proliferation of hepatocytes during liver regeneration. However, conditional deletion of *Yap/Taz* in adult hepatocytes did not noticeably impair liver regeneration after toxic injury or after partial hepatectomy. Considering liver development, we and others found that deletion of *Yap/Taz* in hepatoblasts led to the formation of normal-sized adult livers with normal numbers of hepatocytes[3] and normal zonation, judged by the glutamine synthetase and Cyp2e1 expression patterns. Therefore, *Yap/Taz* are not required in hepatocytes for their proliferation during development or regeneration.

We elucidated the chain of events that lead to the liver regeneration defects in *Yap/Taz* mutant mice. Conditional deletion of *Yap* and *Taz* in BECs of adult mice caused degeneration of the biliary tree[12] and cholestasis. Cholestasis, in turn, impaired the recruitment and activation of macrophages, thereby delaying the clearance of necrotic cell corpses after toxic injury. This model is supported by the findings that cholestasis induced by BDL in wild-type mice or experimental depletion of macrophages phenocopied the regeneration defects of *Yap/Taz*$^{BEC\text{-}KO}$ mutants. Molecularly, we found that *Yap/Taz*$^{BEC\text{-}KO}$ mutant livers had elevated activity of the bile acid receptor PXR, and pharmacologic activation of PXR was sufficient to mimic the regeneration phenotype of *Yap/Taz*$^{BEC\text{-}KO}$ mutants. These preliminary data suggest that bile acid overload impairs the immune response after CCl_4 injury through hyperactivation of PXR, in accordance with other studies describing the anti-inflammatory effects of PXR in the liver and other organs by suppressing the activity of nuclear factor–κB, a key regulator of inflammation and the immune response.[43] We postulate that deletion of *Yap/Taz* in BECs ultimately leads to activation of PXR, which suppresses hepatic cytokine expression and macrophage activity.[43,44] Future experiments in genetic models should be performed to validate these results. Others reported that pharmacologic activation of PXR induced YAP activity in hepatocytes, which caused liver overgrowth and accelerated liver regeneration after partial hepatectomy.[45] This opposite effect of PXR activation on regeneration after partial hepatectomy compared with the inhibitory effect on regeneration after toxic injury in our study can be explained by the use of different regeneration models. In contrast to the partial hepatectomy model, regeneration after toxic liver injury requires clearance of cell debris, which is inhibited by PXR activation, according to our results. In conclusion, YAP and TAZ are required in BECs to maintain bile duct integrity and to prevent the activation of PXR by cholestasis.

A surprising observation in our experiments was that conditional deletion of *Yap* and *Taz* specifically in adult hepatocytes had no noticeable effects on liver regeneration compared with the strong effects caused by *Yap/Taz* deletion in BECs. In contrast, other studies reported that hepatocyte-specific deletion or knockdown of *Yap* in adult mice caused a 16-hour delay in hepatocyte cell cycle re-entry after partial hepatectomy.[9,16] However, we found no significant difference in the onset of proliferation between wild-type and mutant mice after CCl_4 injection. Consistently, Mooring et al[8] reported that hepatocytes from *AAV-Cre Yap/Taz* mutant animals up-regulated basically all of the genes that were induced in wild-type animals after acute CCl_4 injury, although mutant mice developed less fibrosis after chronic CCl_4 injection due

to lower induction of the pro-inflammatory gene Cyr61. However, several studies reported strong regeneration defects in *Yap*, *Taz*, or *Yap/Taz* mutant livers after partial hepatectomy or BDL.[2,7,18] These studies, however, deleted *Yap* and/or *Taz* from hepatoblasts using *Alb-Cre* or from adult hepatocytes and BECs by *Mx1-Cre,* and did not determine the specific requirements for *Yap/Taz* in hepatocytes vs BECs. Therefore, we conclude that *Yap/Taz* are largely dispensable in hepatocytes for the induction of the regeneration program and for regenerative proliferation.

The minimal requirement for YAP/TAZ in hepatocytes during liver regeneration after toxic injury creates a conundrum because YAP/TAZ are transiently activated in hepatocytes in response to liver injury.[2,7–13] Although YAP/TAZ can act redundantly with other signaling pathways that are activated during liver regeneration,[46] YAP/TAZ can also regulate processes that are not easily assayed. For example, YAP/TAZ activation can increase the competitive fitness of noninjured hepatocytes, thereby selecting the fitter cells for proliferation[5,47] or YAP/TAZ can prime hepatocytes for transdifferentiation into liver progenitor cells or BECs.[12] Supporting this hypothesis, hepatocytes around damaged bile ducts induce osteopontin and Sox9 expression,[13] markers for BECs and progenitor cells; ectopic activation of YAP is sufficient to trigger the transdifferentiation of adult hepatocytes into BECs[48]; and YAP/TAZ are required for ectopic proliferation of BECs in ductular reactions, whether they arise from BECs or from hepatocytes.[12,13,49] However, such transdifferentiation of hepatocytes into BECs is not important for the regeneration of CCl_4-induced injuries.[20] Therefore, YAP/TAZ activation might promote hepatocyte plasticity and create the potential for hepatocytes to transdifferentiate, although this potential might not always be utilized for the regeneration of different types of liver injury.

Our data indicate that the cholestasis caused by the defects in bile duct maintenance is the primary driver of the regeneration defects in YAP/TAZ mutants. However, how cholestasis causes defects in liver regeneration is poorly understood. Our observation that depletion of macrophages closely phenocopied the regeneration defects caused by BDL indicates that the suppression of macrophage function is one of the main causes of how cholestasis inhibits liver regeneration after toxic injury. Consistent with this interpretation, cholestatic mice and patients have an impaired immune response and pathogen clearance after bacterial or viral infection.[50–52] In addition, cholestasis affects hepatocyte proliferation, in concordance with our findings, and liver regrowth after partial hepatectomy in mice.[50] Several mechanisms can cause these defects. On the one hand, elevated bile acids can directly impact the function and polarization of macrophages.[53] On the other hand, bile acids can impact hepatocytes directly. In wild-type mice, regenerating hepatocytes not only induced cell proliferation genes, but also genes encoding immune cell activating signals, a central part of the model that hepatocytes are general organizers of liver regeneration.[46] These induced signaling molecules included Ccl2, which is an important attractant for monocytes that mature into macrophages.[37] However, hepatocytes in *Yap/Taz*$^{BEC\text{-}KO}$ mice no longer induced these immune signals, although they still up-regulated the proliferation genes. Thus, the down-regulated cytokine induction can be a major cause of the defects in immune cell recruitment and activation. Yet, macrophages in *Yap/Taz*$^{BEC\text{-}KO}$ mutant livers still activated cell proliferation genes, indicating that they responded to other injury-induced signals. Molecularly, PXR activation can affect hepatocytes and macrophages, as it is expressed in both cell types. Notably, PXR hyperactivation in hepatocytes is sufficient to suppress cytokine expression after chronic CCl_4.[43] Therefore, hyperactivation of PXR in hepatocytes as a result of cholestasis can at least partially explain the suppressed cytokine expression in hepatocytes and the defects in macrophage activation in *Yap/Taz*$^{BEC\text{-}KO}$ mutant mice after toxic injury. Our data further revealed that FXR is marginally more active in mutant livers after CCl_4 injection compared with controls. Therefore, although activation of FXR by physiologic levels of bile acids promotes liver regeneration,[41] FXR modulation seems to play a minor role in inhibiting liver regeneration in *Yap/Taz*$^{BEC\text{-}KO}$ mice.

In summary, our results clarify that YAP and TAZ do not play a cell-autonomous and instructive role in hepatocytes during liver regeneration, but are required in BECs to prevent cholestasis, which causes secondary effects on hepatocytes and macrophages that impair liver regeneration. Our findings have implications for our understanding of the Hippo pathway beyond its role in liver regeneration. In particular, our study urges analysis of the function of the Hippo pathway in a cell-type–specific manner to uncover potentially cell-autonomous vs non–cell-autonomous effects of YAP/TAZ.

Supplementary Material

Note: To access the supplementary material accompanying this article, visit the online version of *Gastroenterology* at www.gastrojournal.org, and at http://dxdoi.org/10.1053/j.gastro.2020.10.035.

References

1. Moya IM, Halder G. Hippo-YAP/TAZ signalling in organ regeneration and regenerative medicine. Nat Rev Mol Cell Biol 2019;20:211–226.
2. Lu L, Finegold MJ, Johnson RL. Hippo pathway coactivators Yap and Taz are required to coordinate mammalian liver regeneration. Exp Mol Med 2018; 50:e423.
3. **Zhang N, Bai H**, David KK, et al. The Merlin/NF2 tumor suppressor functions through the YAP oncoprotein to regulate tissue homeostasis in mammals. Dev Cell 2010; 19:27–38.
4. Fitamant J, Kottakis F, Benhamouche S, et al. YAP inhibition restores hepatocyte differentiation in advanced HCC, leading to tumor regression. Cell Rep 2015; 10:1692–1707.
5. **Moya IM, Castaldo SA, Van den Mooter L**, et al. Peritumoral activation of the Hippo pathway effectors YAP

and TAZ suppresses liver cancer in mice. Science 2019; 366:1029–1034.
6. Yi J, Lu L, Yanger K, et al. Large tumor suppressor homologs 1 and 2 regulate mouse liver progenitor cell proliferation and maturation through antagonism of the coactivators YAP and TAZ. Hepatology 2016;64:1757–1772.
7. **Bai H, Zhang N**, Xu Y, et al. Yes-associated protein regulates the hepatic response after bile duct ligation. Hepatology 2012;56:1097–1107.
8. Mooring M, Fowl BH, Lum SZC, et al. Hepatocyte stress increases expression of YAP and TAZ in hepatocytes to promote parenchymal inflammation and fibrosis. Hepatology 2020;71:1813–1830.
9. **Tschuor C, Kachaylo E**, Ungethüm U, et al. Yes-associated protein promotes early hepatocyte cell cycle progression in regenerating liver after tissue loss. FASEB Bioadv 2019;1:51–61.
10. Fang Y, Liu C, Shu B, et al. Axis of serotonin -pERK-YAP in liver regeneration. Life Sci 2018;209:490–497.
11. Swiderska-Syn M, Xie G, Michelotti GA, et al. Hedgehog regulates yes-associated protein 1 in regenerating mouse liver. Hepatology 2016;64:232–244.
12. **Pepe-Mooney BJ, Dill MT, Alemany A**, et al. Single-cell analysis of the liver epithelium reveals dynamic heterogeneity and an essential role for YAP in homeostasis and regeneration. Cell Stem Cell 2019; 25:23–38.e8.
13. **Planas-Paz L, Sun T**, Pikiolek M, et al. YAP, but Not RSPO-LGR4/5, signaling in biliary epithelial cells promotes a ductular reaction in response to liver injury. Cell Stem Cell 2019;25:39–53.e10.
14. Loforese G, Malinka T, Keogh A, et al. Impaired liver regeneration in aged mice can be rescued by silencing Hippo core kinases MST1 and MST2. EMBO Mol Med 2017;9:46–60.
15. **Fan F, He Z, Kong LL**, et al. Pharmacological targeting of kinases MST1 and MST2 augments tissue repair and regeneration. Sci Transl Med 2016; 8:352ra108.
16. Oh SH, Swiderska-Syn M, Jewell ML, et al. Liver regeneration requires Yap1-TGFβ-dependent epithelial-mesenchymal transition in hepatocytes. J Hepatol 2018;69:359–367.
17. **Su T, Bondar T**, Zhou X, et al. Two-signal requirement for growth-promoting function of Yap in hepatocytes. Elife 2015;4:e02948.
18. Kim AR, Park JI, Oh HT, et al. TAZ stimulates liver regeneration through interleukin-6-induced hepatocyte proliferation and inhibition of cell death after liver injury. FASEB J 2019;33:5914–5923.
19. Weisend CM, Kundert JA, Suvorova ES, et al. Cre activity in fetal albCre mouse hepatocytes: utility for developmental studies. Genesis 2009;47:789–792.
20. Hammad S, Hoehme S, Friebel A, et al. Protocols for staining of bile canalicular and sinusoidal networks of human, mouse and pig livers, three-dimensional reconstruction and quantification of tissue microarchitecture by image processing and analysis. Arch Toxicol 2014; 88:1161–1183.
21. Apte UM. Liver Regeneration: Basic Mechanisms, Relevant Models and Clinical Applications. Amsterdam: Elsevier, 2015.
22. **Cox AG, Hwang KL**, Brown KK, et al. Yap reprograms glutamine metabolism to increase nucleotide biosynthesis and enable liver growth. Nat Cell Biol 2016; 18:886–896.
23. **Lesaffer B, Verboven E**, Van Huffel L, et al. Comparison of the Opn-CreER and Ck19-CreER drivers in bile ducts of normal and injured mouse livers. Cells 2019;8:380.
24. Nakanuma Y, Tsuneyama K, Harada K. Pathology and pathogenesis of intrahepatic bile duct loss. J Hepatobiliary Pancreat Surg 2001;8:303–315.
25. Paulusma CC, Kothe MJ, Bakker CT, et al. Zonal down-regulation and redistribution of the multidrug resistance protein 2 during bile duct ligation in rat liver. Hepatology 2000;31:684–693.
26. Donner MG, Schumacher S, Warskulat U, et al. Obstructive cholestasis induces TNF-alpha- and IL-1 -mediated periportal downregulation of Bsep and zonal regulation of Ntcp, Oatp1a4, and Oatp1b2. Am J Physiol Gastrointest Liver Physiol 2007;293:G1134–G1146.
27. Zhao Q, Yang R, Wang J, et al. PPARα activation protects against cholestatic liver injury. Sci Rep 2017; 7:9967.
28. **Zhang Y, Li F**, Patterson AD, et al. Abcb11 deficiency induces cholestasis coupled to impaired β-fatty acid oxidation in mice. J Biol Chem 2012;287:24784–24794.
29. **Horst AK, Najjar SM**, Wagener C, et al. CEACAM1 in liver injury, metabolic and immune regulation. Int J Mol Sci 2018;19:3110.
30. Shan Z, Ju C. Hepatic macrophages in liver injury. Front Immunol 2020;11:322.
31. Ramachandran P, Pellicoro A, Vernon MA, et al. Differential Ly-6C expression identifies the recruited macrophage phenotype, which orchestrates the regression of murine liver fibrosis. Proc Natl Acad Sci U S A 2012; 109:E3186–E3195.
32. Scott CL, Zheng F, De Baetselier P, et al. Bone marrow-derived monocytes give rise to self-renewing and fully differentiated Kupffer cells. Nat Commun 2016;7:10321.
33. Caruso RA, Branca G, Fedele F, et al. Mechanisms of coagulative necrosis in malignant epithelial tumors (review). Oncol Lett 2014;8:1397–1402.
34. Li M, Sun X, Zhao J, et al. CCL5 deficiency promotes liver repair by improving inflammation resolution and liver regeneration through M2 macrophage polarization. Cell Mol Immunol 2020;17:753–764.
35. Lawrence T, Natoli G. Transcriptional regulation of macrophage polarization: enabling diversity with identity. Nat Rev Immunol 2011;11:750–761.
36. Jablonski KA, Amici SA, Webb LM, et al. Novel markers to delineate murine M1 and M2 macrophages. PLoS One 2015;10:e0145342.
37. Saiman Y, Friedman SL. The role of chemokines in acute liver injury. Front Physiol 2012;3:213.
38. Schaap FG, Trauner M, Jansen PL. Bile acid receptors as targets for drug development. Nat Rev Gastroenterol Hepatol 2014;11:55–67.

39. Staudinger J, Liu Y, Madan A, et al. Coordinate regulation of xenobiotic and bile acid homeostasis by pregnane X receptor. Drug Metab Dispos 2001;29:1467–1472.
40. Chai J, Luo D, Wu X, et al. Changes of organic anion transporter MRP4 and related nuclear receptors in human obstructive cholestasis. J Gastrointest Surg 2011; 15:996–1004.
41. Huang W, Ma K, Zhang J, et al. Nuclear receptor-dependent bile acid signaling is required for normal liver regeneration. Science 2006;312:233–236.
42. Brobst DE, Ding X, Creech KL, et al. Guggulsterone activates multiple nuclear receptors and induces CYP3A gene expression through the pregnane X receptor. J Pharmacol Exp Ther 2004;310:528–535.
43. Wallace K, Cowie DE, Konstantinou DK, et al. The PXR is a drug target for chronic inflammatory liver disease. J Steroid Biochem Mol Biol 2010;120:137–148.
44. Hu G, Xu C, Staudinger JL. Pregnane X receptor is SUMOylated to repress the inflammatory response. J Pharmacol Exp Ther 2010;335:342–350.
45. Jiang Y, Feng D, Ma X, et al. Pregnane X receptor regulates liver size and liver cell fate by Yes-associated protein activation in mice. Hepatology 2019;69:343–358.
46. Michalopoulos GK. Liver regeneration. J Cell Physiol 2007;213:286–300.
47. Hashimoto M, Sasaki H. Epiblast formation by TEAD-YAP-dependent expression of pluripotency factors and competitive elimination of unspecified cells. Dev Cell 2019;50:139–154.
48. **Yimlamai D, Christodoulou C**, Galli GG, et al. Hippo pathway activity influences liver cell fate. Cell 2014; 157:1324–1338.
49. **Li W, Yang L**, He Q, et al. A homeostatic Arid1a-dependent permissive chromatin state licenses hepatocyte responsiveness to liver-injury-associated YAP signaling. Cell Stem Cell 2019;25:54–68.
50. Yokoyama Y, Nagino M, Nimura Y. Mechanism of impaired hepatic regeneration in cholestatic liver. J Hepatobiliary Pancreat Surg 2007;14:159–166.
51. Jeyarajah DR, Kielar ML, Saboorian H, et al. Impact of bile duct obstruction on hepatic *E. coli* infection: role of IL-10. Am J Physiol Gastrointest Liver Physiol 2006; 291:G91–G94.
52. **Lang E, Pozdeev VI, Shinde PV**, et al. Cholestasis induced liver pathology results in dysfunctional immune responses after arenavirus infection. Sci Rep 2018; 8:12179.
53. Wammers M, Schupp AK, Bode JG, et al. Reprogramming of pro-inflammatory human macrophages to an anti-inflammatory phenotype by bile acids. Sci Rep 2018;8:255.

Author names in bold designate shared co-first authorship.

Received December 3, 2019. Accepted October 19, 2020.

Correspondence
Address correspondence to: Georg Halder, PhD, Vlaams Instituut voor Biotechnologie-Katholieke Universiteit Leuven Center for Cancer Biology, Department of Oncology, Katholieke Universiteit Leuven, Herestraat 49-bus 912, 3000 Leuven, Belgium. e-mail: georg.halder@vib.be.

Acknowledgments
Anti-Mrp-2 and anti-Bsep antibodies were a generous gift of Professor Bruno Stieger (University of Zurich, Switzerland). The authors thank Jean-Christoph Marine and Randy Johnson for sending mouse strains.

The Gene Expression Omnibus accession number for the RNA-sequencing data sets reported in this article is GSE157088.

CRediT Authorship Contributions
Elisabeth Verboven, MS (Data curation: Lead; Formal analysis: Lead; Investigation: Lead; Methodology: Lead; Project administration: Lead; Validation: Lead; Visualization: Lead; Writing – original draft: Equal; Writing – review & editing: Equal).

Iván M. Moya, PhD (Conceptualization: Lead; Investigation: Supporting; Methodology: Supporting; Supervision: Equal; Visualization: Supporting; Writing – original draft: Equal; Writing – review & editing: Supporting).

Leticia Sansores-Garcia, MS (Investigation: Supporting; Methodology: Supporting).

Jun Xie, PhD (Investigation: Supporting).

Hanne Hillen, MS (Investigation: Supporting).

Weronika Kowalczyk, MS (Investigation: Supporting; Bio-informatics analysis: Lead).

Gerlanda Vella, MS (Investigation: Supporting; Methodology: Supporting; Flow cytometry expertise: Lead).

Stefaan Verhulst, PhD (Methodology: Supporting; Bile duct ligation and cell isolations: Lead).

Stephanie A. Castaldo, MS (Investigation: Supporting).

Ana Algueró-Nadal, MS (Investigation: Supporting).

Lucia Romanelli, PhD (Investigation: Supporting).

Cristina Mercader-Celma, BS (Investigation: Supporting).

Natália A. Souza, MS (Investigation: Supporting).

Soheil Soheily, MS (Investigation: Supporting).

Leen van Huffel, MS (Investigation: Supporting; Resources: Supporting).

Thomas Van Brussel, PhD (RNA-sequencing: Lead).

Diether Lambrechts, PhD (RNA-sequencing: Supporting).

Tania Roskams, MD, PhD (Investigation: Supporting; Conceptual advice: Supporting).

Frédéric P. Lemaigre, PhD (conceptual advice and manuscript review: Supporting).

Gabrielle Bergers, PhD (Investigation: Supporting; Methodology: Supporting).

Leo A. van Grunsven, PhD (Conceptual advice and manuscript review: Supporting).

Georg Halder, PhD (Conceptualization: Supporting; Funding acquisition: Lead; Supervision: Equal; Writing – original draft: Equal; Writing – review & editing: Equal).

Conflicts of interest
The authors disclose no conflicts.

Funding
Elisabeth Verboven, Stéphanie A. Castaldo, Weronika Kowalczyk, and Ana Algueró-Nadal were supported by a doctoral fellowship from the Research Foundation Flanders (FWO). This work was supported by grants from Stichting tegen Kanker and the FWO to Georg Halder.